A.J.H. thanks the Advanced Study Program of the National Center for Atmospheric Research (NCAR) for providing a Graduate Research Assistantship. NCAR is supported by the National Science Foundation. J.W.B. thanks the John Simon Gugenheim Foundation for a fellowship. We are especially grateful to Jose Rodriguez, Malcolm Ko, and N. Dak Sze for providing the model calculations. We thank Susan Solomon and Bob Watson for helpful discussions of this work.

Registry No. BrO, 15656-19-6; ClO, 14989-30-1.

Photodissociation of the Hydrogen-Bonded Heterodimer Ion $[C_6H_5OH–NH_3]^+$

Naohiko Mikami,* Akihiro Okabe, and Itaru Suzuki

Department of Chemistry, Faculty of Science, Tohoku University, Sendai 980, Japan
(Received: August 12, 1987)

Photodissociation of the hydrogen-bonded heterodimer ion $[C_6H_5OH–NH_3]^+$ has been studied following the selective photoionization of the jet-cooled dimer via its S_1 state by using two-color multiphoton ionization technique. From the mass-selected photoionization yield spectrum for generation of the dimer ion, the adiabatic ionization potential of $C_6H_5OH–NH_3$ was found to be 62 200 ± 100 cm^{-1} (ca. 7.71 eV). It was found that the fragment ion $C_6H_5OH^+$ is generated by the photoionization of the dimer with the ionization energy higher than a threshold at 70 400 cm^{-1}, whereas only the dimer ion is generated with the photoionization energy lower than the threshold. Dissociation energy of the dimer ion due to $[C_6H_5OH–NH_3]^+ \rightarrow C_6H_5OH^+ + NH_3$ was found to be 8200 ± 150 cm^{-1}. No NH_4^+ production was found even when the photoionization energy exceeded the expected threshold for the NH_4^+ generation. The selective dissociation producing the phenol ion is discussed in relation to the structure of the dimer ion.

Introduction

Photodissociation of the hydrogen bond represents an important class of unimolecular photochemical processes in hydrogen-bonded dimers or clusters in the gas phase. The dissociation of cations of hydrogen-bonded dimers is of particular interest concerning proton transfer. In this respect, the dissociation of a dimer cation, $[AH]_2^+$, is expected to occur in two ways: one is to generate the protonated fragment ion AH_2^+ and the other produces the unprotonated fragment ion AH^+. Both fragment ions are frequently observed in photoionization mass spectroscopic studies of the hydrogen-bonded clusters.[1-7] These extensive studies show that the protonated ion is originated from the photoionized clusters. The dissociation accompanied by the proton transfer occurring in cluster ions results in efficient production of the protonated ion. Several studies on ion–molecule reactions within cluster ions have recently been done, showing a variety of reaction products.[8,9] On the other hand, the origin of the unprotonated ion has not been well understood. Since ordinary cluster sources such as molecular beams or supersonic free expansions necessarily contain a large number of monomer molecules, a mixture of clusters and the monomer AH are subject to the photoionization. In most cases of photoionization mass spectroscopic studies of the clusters, the photoionization is performed by using vacuum-UV light whose photon energy is sufficiently larger than the ionization potential (IP) of AH. A large number of AH^+ ions generated directly from AH, then, are indistinguishable from the same ionic species produced by the dissociation of the cluster ions if it occurs. Therefore, the identification of the dissociation process producing the unprotonated AH^+ ion is quite difficult with this photoionization method.

In this paper, we report a photodissociation study of the cation of the hydrogen-bonded complex of phenol with ammonia under an isolated molecular condition prepared in a supersonic free expansion. We have employed the stepwise photoionization method using the two-color multiphoton ionization technique,[10] where the complex is initially excited to its first singlet S_1 excited state and subsequently photoionized to its cation state. Since the formation energy of the hydrogen bond of the complex in the S_1 state is generally different from that in the ground S_0 state, the $S_1 \leftarrow S_0$ excitation energy of the complex differs from the corresponding energy of other species. In the stepwise photoionization via the S_1 state, therefore, the selective ionization of the complex is allowed without ionizing other species which are included in the free expansion.

The complex of $C_6H_5OH–NH_3$ is a hydrogen-bonded heterodimer, whose cation may dissociate in one of three ways:

$$[C_6H_5OH–NH_3]^+ \rightarrow C_6H_5OH^+ + NH_3 \quad (1)$$

$$\rightarrow C_6H_5O + NH_4^+ \quad (2)$$

$$\rightarrow C_6H_5OH + NH_3^+ \quad (3)$$

The purpose of this work is to find the major dissociation pathway of the dimer ion among the three dissociation channels above when we put excess energies into the dimer ion during the photoionization. Especially we are interested in the problem of whether the dissociation is accompanied by the proton transfer or not. In a previous work,[11] we reported a photodissociation study of the jet-cooled phenol–trimethylamine dimer ion, $[C_6H_5OH–N(CH_3)_3]^+$, which was found to dissociate efficiently into C_6H_5O

(1) Ng, C. Y.; Trevor, D. J.; Tiedemann, P. W.; Ceyer, S. T.; Kronebusch, P. L.; Mahan, B. H.; Lee, Y. T. *J. Chem. Phys.* **1977**, *67*, 4235.
(2) Ceyer, S. T.; Tiedemann, P. W.; Mahan, B. H.; Lee, Y. T. *J. Chem. Phys.* **1979**, *70*, 14.
(3) Echt, O.; Morgan, S.; Dao, P. D.; Stanley, R. J.; Castleman, A. W., Jr. *Ber. Bunsen-Ges. Phys. Chem.* **1984**, *88*, 217.
(4) Shinohara, H.; Nishi, N.; Washida, N. *J. Chem. Phys.* **1985**, *83*, 1939.
(5) Echt, O.; Dao, P. D.; Morgan, S.; Castleman, A. W., Jr. *J. Chem. Phys.* **1985**, *82*, 4076.
(6) Hermann, V.; Kay, B. D.; Castleman, A. W., Jr. *Chem. Phys.* **1982**, *72*, 185.
(7) Castleman, A. W., Jr.; Echt, O.; Morgan, S.; Dao, P. D.; Stanley, R. J. *Ber. Bunsen-Ges. Phys. Chem.* **1985**, *89*, 281.
(8) Garvey, J. F.; Bernstein, R. B. *Chem. Phys. Lett.* **1986**, *126*, 394; *J. Phys. Chem.* **1986**, *90*, 3577.
(9) Schriver, K. E.; Camarena, A. M.; Hahn, M. Y.; Paguia, A. J.; Whetten, R. L. *J. Phys. Chem.* **1987**, *91*, 1786.
(10) Gonohe, N.; Abe, H.; Mikami, N.; Ito, M. *J. Phys. Chem.* **1985**, *89*, 3642.
(11) Mikami, N.; Suzuki, I.; Okabe, A. *J. Phys. Chem.* **1987**, *91*, 5242.

0022-3654/88/2092-1858$01.50/0

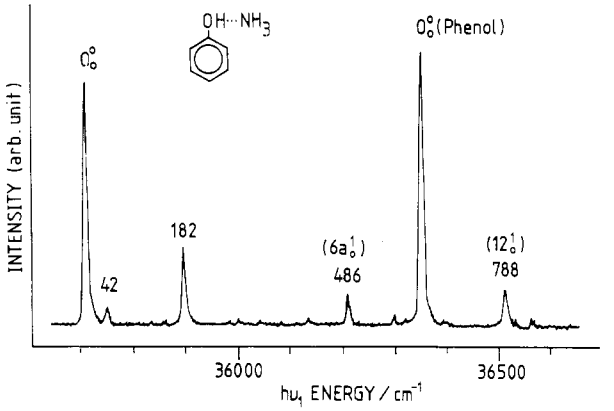

Figure 1. MPI spectrum of the $S_1 \leftarrow S_0$ transition of jet-cooled C_6H_5-$OH-NH_3$. The 0,0 transition occurs at 35 717 ± 2 cm^{-1}, which is 635 cm^{-1} lower than the 0,0 transition of phenol (36 352 cm^{-1}).

and $HN(CH_3)_3^+$. The generation of the protonated fragment $HN(CH_3)_3^+$ was found to be due to the proton transfer within the dimer ion prior to the dissociation. It is also interesting to see that the dissociation process in the $[C_6H_5OH-NR_3]^+$ system may be affected by the difference in proton affinity of the proton acceptor NR_3 (R = H, CH_3) for the hydrogen bond.

In order to characterize the S_1 and S_0 dimer, the fluorescence excitation and dispersed fluorescence spectra are also observed and analyzed.

Experimental Section

The hydrogen-bonded dimer was prepared by a pulsed supersonic free expansion of a gaseous mixture of C_6H_5OH and NH_3 seeded in helium gas at 3 atm. The partial pressures of C_6H_5OH and NH_3 were about 10 and 45 Torr, respectively. The fluorescence excitation and dispersed fluorescence spectra of the jet-cooled dimer were obtained by an apparatus reported elsewhere.[12] Details of the experimental setup for the mass-selected two-color photoionization spectroscopy were described in a previous paper.[11] The second harmonic of a dye laser (Lambda Physik, FL-2002, Coumarin 540 A, KDP) pumped by a XeCl excimer laser (Lambda Physik, EMG 102 MSC) was used as a light source (ν_1) for the $S_1 \leftarrow S_0$ excitation of the dimer. The fundamental output and its second harmonic of another dye laser (Molectron, DL-14) pumped by the same XeCl laser were used as a photoionization light source (ν_2) and were scanned to obtain the photoionization yield spectrum. Both light beams ν_1 and ν_2 were led into a vacuum chamber in opposite directions from each other and coaxially focused by lenses into the free jet 20 mm downstream from a nozzle having an orifice of 0.8-mm diameter. Cations generated by the photoionization were repelled from the ionization region by a positively charged plate into an entrance of a quadrupole mass filter (Extranuclear 4-270-9) and detected by a channel electron multiplier (Murata, Ceratron). The ion-current intensity was normalized with respect to the power spectrum of ν_2 which was simultaneously monitored by a photomultiplier.

Results

Characterization of the S_1 and S_0 Dimer. Figure 1 shows the one-photon-resonant two-photon-ionization (MPI) spectrum of the jet-cooled dimer in the region of the origin of the $S_1 \leftarrow S_0$ transition, obtained by monitoring the total ion current. We also observed the fluorescence excitation spectrum of the jet-cooled dimer. The fluorescence excitation spectrum is essentially the same as the MPI spectrum except for several extra bands due to the complex with water, which could not be removed completely from the gaseous mixture.[13] An intense band at 35 717 cm^{-1} is assigned

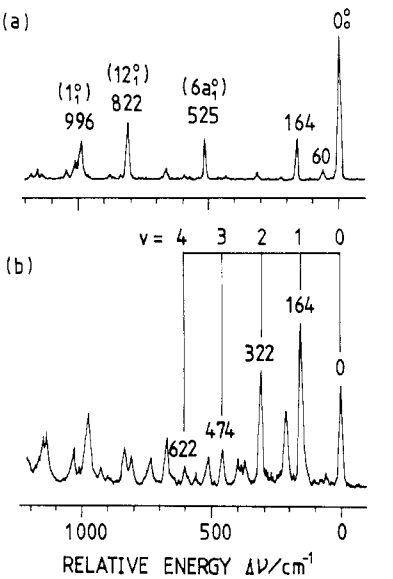

Figure 2. Dispersed fluorescence spectra of jet-cooled $C_6H_5OH-NH_3$, obtained by excitations of (a) the 0,0 and (b) the 0 + 182-cm^{-1} transitions shown in Figure 1. The quantum numbers of the intermolecular stretching vibration and the relative energy spacings from the origin are indicated in (b).

to the 0,0 transition of the dimer. A large red shift of 635 cm^{-1} from the 0,0 transition of free phenol (36 352 cm^{-1}) shows that phenol acts as a proton donor and ammonia as a proton acceptor in the hydrogen bonding.[14] The bands at 0 + 42 and 0 + 182 cm^{-1} are assigned as vibronic bands involving vibrations of hydrogen-bond modes. The bands at 0 + 486 and 0 + 788 cm^{-1} are assigned to the vibronic bands involving vibrations of the phenol moiety. They correspond well to the vibronic bands of 0 + 476 ($6a^1$) and 0 + 783 (12^1) cm^{-1} of free phenol.[15] The good correspondence shows that the S_1 excitation of the dimer is characteristic of the local excitation of the phenol moiety and the proton transfer is not involved in S_1.

Figure 2 shows the dispersed fluorescence spectra of the dimer obtained by the excitation of the 0,0 and 0 + 182 cm^{-1} bands. The prominant bands in spectrum a in the figure are readily assigned to bands coupled with vibrations of phenol of 525, 822, and 996 cm^{-1} [16] and hydrogen-bond modes whose fundamental frequencies are 60 and 164 cm^{-1}. By analogy with the frequency of known hydrogen-bond modes,[17] the 164-cm^{-1} vibration is assigned to the fundamental vibration of the hydrogen-bond stretching mode in the S_0 state. In spectrum b obtained by the excitation of the 0 + 182 cm^{-1} band, a progression of the stretching vibration appears up to the fourth quantum. The progression of the stretching vibration is enhanced owing to the better Franck–Condon factors to the S_0 state from the first quantum state of the vibration in S_1. Other bands are due to the similar progressions starting from the 60-cm^{-1} band and the bands of the phenol modes. The frequency difference between the adjacent members in the progression decreases with increase of the quantum number, showing an anharmonicity of the stretching vibration. The energy level $G(v)$ of the vth quantum of this vibration is expressed by

$$G(v) = 170(v + \tfrac{1}{2}) - 3.0(v + \tfrac{1}{2})^2 \quad (\text{in } cm^{-1}) \qquad (4)$$

Assuming a Morse-type function for the one-dimensional dissociative potential of the stretching vibration, the dissociation energy $D_e(S_0)$ of the hydrogen bond can be estimated by using the harmonic and anharmonic coefficients of (4). The estimated

(12) Mikami, N.; Hiraya, A.; Fujiwara, I.; Ito, M. *Chem. Phys. Lett.* **1980**, *74*, 531.

(13) This indicates that there are small amounts of many species other than the phenol–ammonia dimer in the present nozzle source, although they do not clearly appear in the MPI spectrum.

(14) Abe, H.; Mikami, N.; Ito, M. *J. Phys. Chem.* **1982**, *86*, 1768.

(15) Bist, H. D.; Brand, J. C. D.; Williams, D. R. *J. Mol. Spectrosc.* **1967**, *24*, 413.

(16) Bist, H. D.; Brand, J. C. D.; Williams, D. R. *J. Mol. Spectrosc.* **1967**, *24*, 402.

(17) Abe, H.; Mikami, N.; Ito, M.; Udagawa, Y. *J. Phys. Chem.* **1982**, *86*, 2567.

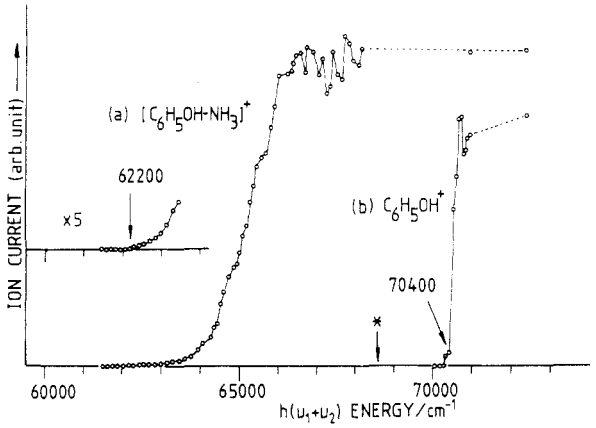

Figure 3. (a) Two-color photoionization yield spectrum for the $[C_6H_5OH\text{-}NH_3]^+$ ion current, where the $S_1(0^0)$ level was excited with ν_1 fixed at 35 717 cm^{-1} and ν_2 was scanned for the photoionization. The enhanced yield spectrum (×5) near the threshold is given. (b) Threshold spectrum for the appearance of $C_6H_5OH^+$ resulting from the dissociation $[C_6H_5OH\text{-}NH_3]^+ \rightarrow C_6H_5OH^+ + NH_3$. $S_1(0^0)$ of the dimer was excited with ν_1, and the $C_6H_5OH^+$ ion current was monitored. Normalization of both ion currents with respect to the ν_2 laser power spectrum was carried out by a point-by-point method. Unnormalized points at the highest energy at 72 400 cm^{-1} are also indicated, where the current intensity of the dimer ion is merely leveled to the normalized yield at the low-energy side. The asterisk indicates the ionization energy of phenol itself (see ref 10).

$D_e(S_0)$ is 2300 ± 500 cm^{-1}. The large error in $D_e(S_0)$ is due to an uncertainty (±1 cm^{-1}) of the anharmonic coefficient. The dissociation energy of the S_1 dimer, $D_e(S_1)$, is readily obtained to be 2935 ± 500 cm^{-1} by taking the sum of $D_e(S_0)$ and the red shift of 635 cm^{-1} in the $S_1 \leftarrow S_0$ excitation spectrum.

Photoionization of the Dimer and Dissociation of the Dimer Ion. Curve a in Figure 3 represents the photoionization yield spectrum of the dimer ion generation, where ν_1 is fixed at the 0,0 band of the $S_1 \leftarrow S_0$ transition of the neutral dimer and ν_2 is scanned for the ionization of the S_1 dimer. The yield spectrum shows an onset at 62 200 ± 100 cm^{-1} and a monotonous increse of the yield going to the higher energy side from the onset. The rather distinct onset of the yield spectrum of $C_6H_5OH\text{-}NH_3$ dimer is in contrast to the case of $C_6H_5OH\text{-}N(CH_3)_3$ dimer,[11] which exhibits a vague onset. The threshold energy is regarded as the adiabatic ionization potential of $C_6H_5OH\text{-}NH_3$ dimer, IP(0) = 62 200 ± 100 cm^{-1}. Since IP(0) of C_6H_5OH is known to be 68 600 ± 10 cm^{-1},[10,18] the difference of 6400 cm^{-1} in IP(0) between phenol and the dimer represents a stabilization energy due to the dimer formation in the ionic state. By taking the sum of the difference and $D_e(S_0)$, the dissociation energy of the dimer ion for the dissociation pathway of (1), D_e(ion), is found to be 8700 ± 600 cm^{-1}.

In the higher energy region of the yield spectrum we have found the $C_6H_5OH^+$ ion produced by the dissociation of the dimer ion, as shown by curve b in Figure 3, which represents the threshold spectrum for the appearance of $C_6H_5OH^+$ (M = 94). The appearance energy (AE) of $C_6H_5OH^+$ generated by the dissociation pathway of (1) is, then, found to be 70 400 ± 50 cm^{-1} by taking the onset of the rise of curve b.

Figure 4 shows the mass spectra obtained by the selective photoionization of the dimer with two different photoionization energies. When the dimer is ionized with the total photon energy of 62 700 cm^{-1}, which is about 500 cm^{-1} above the ionization threshold of the dimer, only the dimer ion $[C_6H_5OH\text{-}NH_3]^+$ (M = 111) is observed as shown in Figure 4a. This mass pattern does not change by increasing the ionization energy up to 70 400 cm^{-1}. By the photoionization with the total photon energy of 71 100 cm^{-1}, which is about 700 cm^{-1} higher than AE of $C_6H_5OH^+$, the photodissociated $C_6H_5OH^+$ (M = 94) is observed as shown in Figure 4b. It is worth noting here that no NH_3^+ ion (M = 17) nor NH_4^+ ion (M = 18) is identified under a signal-to-noise ratio of the mass spectra, which is found to be about 20. The mass spectrum similar to that in Figure 4b is obtained with the photoionization energy of 72 400 cm^{-1}, which is reached by the two-photon ionization via the 0 + 486 cm^{-1} level at 36 203 cm^{-1}, shown in Figure 1. In the present work the further increase of the photoionization energy is restricted by the following reasons. (i) The excitation of the 12^1 vibronic level of the S_1 dimer (at 36 505 cm^{-1} in Figure 1) leads to the extensive vibrational relaxation,[17] so that the photoionization via this level may not gain more excess energy than the expected. (ii) As the photon energy of the ionizing light ν_2 is increased to more than 36 700 cm^{-1}, the ν_2 photon also excites various vibronic states of the dimer and of phenol, causing an experimental difficulty for the selective excitation of the dimer ion.

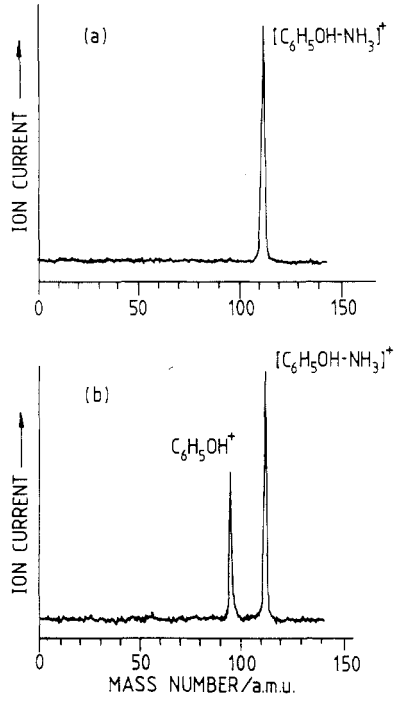

Figure 4. Mass spectra after photoionization of $C_6H_5OH\text{-}NH_3$. Photoionization energies $h(\nu_1+\nu_2)$ with the fixed $h\nu_1$ at 35 717 cm^{-1} are (a) 62 700 and (b) 71 100 cm^{-1}, respectively.

Discussion

Figure 5 shows the energy correlation diagram of the C_6H_5OH and NH_3 system. The dissociation limit producing $C_6H_5OH^*$ and NH_3 corresponds to the $S_1 \leftarrow S_0$ transition energy (4.506 eV) of C_6H_5OH molecule. The dissociation limit of the dimer ion producing $C_6H_5OH^+$ and NH_3 is given by IP(0) of C_6H_5OH (8.505 eV). Another dissociation limit producing C_6H_5O and NH_4^+ is obtained to be 8.49 ± 0.1 eV with respect to the ground state of the C_6H_5OH and NH_3 system by taking the sum of enthalpy changes of the gas-phase reactions

$$C_6H_5OH \rightarrow C_6H_5O + H \qquad \Delta H = +3.74 \pm 0.1 \text{ eV}^{19} \qquad (5)$$

$$H \rightarrow H^+ + e^- \qquad \Delta H = \text{IP}(0) = +13.60 \text{ eV}^{20} \qquad (6)$$

$$NH_3 + H^+ \rightarrow NH_4^+ \qquad \Delta H = -\text{PA} = -8.85 \text{ eV}^{21} \qquad (7)$$

where PA represents the absolute proton affinity. It is to be emphasized that the dissociation limit producing NH_4^+ is very close to that producing $C_6H_5OH^+$ even if the experimental uncertainty (±0.1 eV) in (5) is taken into account. The dissociation

(18) Kimura, K.; Katsumata, S.; Achiba, Y.; Yamazaki, T.; Iwata, S. *Handbook of He I Photoionization Spectra of Fundamental Organic Molecules*; Japan Scientific Societies Press/Halsted Press: Tokyo/New York, 1981.

(19) DeFrees, D. J.; McIver, R. T., Jr.; Hehre, W. J. *J. Am. Chem. Soc.* **1980**, *102*, 3334.

(20) Robinson, J. W. *Handbook of Spectroscopy*; CRC Press, Boca Raton, FL, 1974; Vol. 1.

(21) Aue, D. H.; Bowers, M. T. *Gas Phase Ion Chemistry*; Bowers, M. T., Ed.; Academic: New York, 1979; Vol. 2.

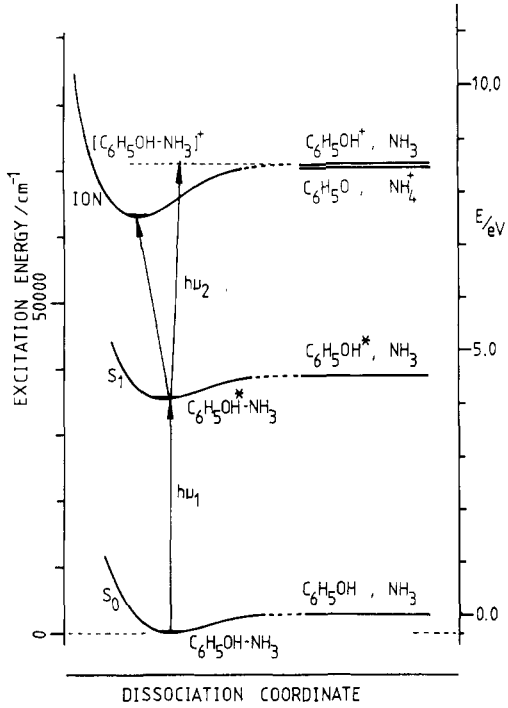

Figure 5. Energy diagram of the C_6H_5OH and NH_3 system. Dissociation energies of the S_0 and S_1 neutral dimer and of the dimer ion are taken to be 1800 ± 50, 2435 ± 50, and 8200 ± 150 cm^{-1}, respectively.

limit producing NH_3^+ corresponds to IP(0) of NH_3 (10.16 eV).[18] It is so high in energy that the possibility of the NH_3^+ production represented by (3) can be neglected in the present work.

Energy correlation between those dissociation limits and the corresponding states of the dimer and its ion can be made by knowing D_e in each state. We have obtained the $D_e(S_0)$ of the neutral dimer from the fluorescence spectrum, as described in a previous section. However, $D_e(S_0)$ obtained from the anharmonic progression in the fluorescence spectrum may not be very accurate because the Morse-type function has been assumed for the potential energy curve. On the other hand, the appearance energy (AE) of $C_6H_5OH^+$ ion generated from the $[C_6H_5OH-NH_3]^+$ ion provides us with more accurate values of D_e of the dimer system. It is clear that AE of $C_6H_5OH^+$ corresponds to the dissociation limit at 8.505 eV on the right-hand-side scale in Figure 5. Therefore, the difference between the AE (70 400 cm^{-1}) of $C_6H_5OH^+$ ion and IP(0) (68 600 cm^{-1}) of C_6H_5OH represents the stabilization energy of the S_0 dimer formation, $D_e(S_0)$. Thus we have obtained a more accurate value of $D_e(S_0)$ = 1800 ± 50 cm^{-1}. $D_e(S_1)$ and D_e(ion) are accordingly determined to be 2435 ± 50 and 8200 ± 150 cm^{-1}, respectively, and these values are adopted in the figure. The agreement between D_e(ion) estimated from the AE of $C_6H_5OH^+$ and that from the fluorescence spectrum indicates that there is no potential energy barrier for the dissociation pathway of (1).

The accurate values of D_e are also useful to fix the dissociation limit producing the NH_4^+ ion with respect to the S_0 neutral dimer. The dissociation limit for the NH_4^+ production (8.49 ± 0.1 eV on the right-hand-side scale in Figure 5) then must lie at 70 280 ± 800 cm^{-1} above the S_1 neutral dimer. Since the dissociation limit is very close to the limit for the $C_6H_5OH^+$ generation, one can naturally expect the NH_4^+ generation in addition to the $C_6H_5OH^+$ generation with the photoionization energy higher than these limits. As described in a previous section, however, no NH_4^+ ion is observed with the photoionization energy of 71 100 cm^{-1} via the zero-point level of the S_1 dimer. No NH_4^+ generation is found even with the photoionization energy of about 72 400 cm^{-1}, which is reached by the ionization via the 0 + 486($6a^1$) level of the S_1 dimer. We conclude therefore that the dissociation producing the unprotonated fragment ion, $C_6H_5OH^+$, occurs in preference to that producing the protonated fragment ion, NH_4^+, in the low-energy dissociation of $[C_6H_5OH-NH_3]^+$.

This preferential generation of the unprotonated fragment ion may be closely related to the shape of the potential energy surface of the dimer ion with respect to the two different dissociation pathways of (1) and (2). Since the photoionization from the S_1 dimer produces the Franck–Condon (FC) states of the ground-state dimer ion, the dissociation from the FC states takes place in competition with the intramolecular vibrational redistribution (IVR) occurring in the dimer ion. This can be confirmed from the mass spectrum given in Figure 4b, where the dimer ion survives even though the photoionization energy exceeds the dissociation limits. This fact indicates that the photogenerated dimer ion is not consumed completely by the dissociation producing $C_6H_5OH^+$ but is preserved partly by the IVR which competes with the dissociation. The dissociation rate is, therefore, not very much larger than the IVR rate. This means that the excess energy of the photogenerated dimer ion is partitioned statistically or quasi-statistically into many vibrational degrees of freedom including the specific dissociation coordinates. Since there is no potential barrier for the $C_6H_5OH^+$ generation, the energy partition to the dissociation pathway of (1) leads to the dissociation from the FC states located above the dissociation limit. The simultaneous generation of the dimer ion and $C_6H_5OH^+$ is thus explained as a result of the extensive IVR from the FC states. In this respect, if there is no potential barrier for the NH_4^+ generation, the IVR also opens the dissociation pathway of (2). However, the experimental result shows that such an energy partition for the NH_4^+ generation does not occur from the FC states. The preferential generation of $C_6H_5OH^+$ over the NH_4^+ generation, therefore, suggests that there is a potential barrier for the dissociation pathway of (2). The barrier height may be higher than the available excess energy of the FC states. In the present work, we do not find the NH_4^+ generation with the photoionization energy up to 72 400 cm^{-1}, so that the barrier height is higher than 2100 cm^{-1} with respect to the limit for NH_4^+ at 8.49 eV. Since the S_1 neutral dimer, as stated above, is the non-proton (hydrogen) transfer form $C_6H_5OH^*-NH_3$ and the photoionization is a very fast process occurring within a time scale of about 10^{-15} s, the FC state of the dimer ion generated from the S_1 dimer seems to be characteristic of phenol ion bound by NH_3, that is, $C_6H_5OH^+-NH_3$. For the NH_4^+ generation the proton transfer is needed prior to the dissociation. The potential barrier for the NH_4^+ generation is due presumably to the promotion energy required for the proton transfer in the hydrogen-bonded dimer ion.

Since the systems of $C_6H_5OH^+$ and NH_3 and of C_6H_5O and NH_4^+ are almost isoenergetic, it is not obvious which of $C_6H_5OH^+-NH_3$ and $C_6H_5O-NH_4^+$ is the most stable form of the dimer ion. As for the low energy photodissociation processes, however, the photoionization produces the non-proton-transfer form $C_6H_5OH^+-NH_3$ and the subsequent dissociation takes place without the proton transfer. In other words, the ion–molecule reaction within the dimer ion is not promoted. This is in contrast to the case of the ion of the hydrogen-bonded dimer of C_6H_5OH and $N(CH_3)_3$.[11] In this dimer ion the dissociation leads to the efficient generation of $HN(CH_3)_3^+$ which was explained by the dissociation of the proton-transfer form $C_6H_5O-HN(CH_3)_3^+$. In this case the ion–molecule reaction within the dimer ion actually occurs during the photoionization–dissociation process. The difference in photodissociation characteristics between the $[C_6H_5OH-NH_3]^+$ and the $[C_6H_5OH-N(CH_3)_3]^+$ ions comes from the difference in their stable forms, which may be presumably determined by proton affinities of NH_3 and $N(CH_3)_3$. The proton affinity of NH_3 is about 0.83 eV less than that of $N(CH_3)_3$,[21] so that the proton-transfer form is less stable in $[C_6H_5OH-NH_3]^+$ than in $[C_6H_5OH-N(CH_3)_3]^+$.[22]

In conclusion, the selective ionization using the two-color multiphoton excitation technique is quite useful for the photo-

(22) With the difference of proton affinity in mind, we tried to study the photodissociation of $[C_6H_5OH-NH_2CH_3]^+$ and of $[C_6H_5OH-NH(CH_3)_2]^+$. At present we have failed to obtain a sufficient amount of the (1:1) heterodimers because of the heavy aggregation of the amine itself.

dissociation studies of cluster ions, and the major dissociation pathway of $[C_6H_5OH-NH_3]^+$ is due to the unprotonated fragment generation expressed by (1).

Acknowledgment. We are grateful to Prof. Mitsuo Ito for stimulating discussions and encouragement during this work. We also thank Dr. T. Ebata for helpful discussions.

Registry No. C_6H_5OH, 108-95-2; NH_3, 7664-41-7; $C_6H_5OH^+$, 40932-22-7.

Absorption Cross Sections and Kinetic Considerations of the IO Radical As Determined by Laser Flash Photolysis/Laser Absorption Spectroscopy

R. E. Stickel,† A. J. Hynes,‡ J. D. Bradshaw, W. L. Chameides, and D. D. Davis*

School of Geophysical Sciences, Georgia Institute of Technology, Atlanta, Georgia 30332
(Received: August 18, 1987)

Independent measurements of the absorption cross section of the IO radical for the $A^2\Pi-X^2\Pi$ band system are reported. A value of $(3.1 \pm 0.6) \times 10^{-17}$ cm^2 was observed for the (4,0) bandhead in good agreement with an earlier investigation. Results are also reported for the (5,0), (3,0), (2,0), and (1,0) bands over the wavelength range of 410–470 nm. However, no measurable ($<2 \times 10^{-18}$ cm^2) absorption was found for the (0,0) band. The atmospheric photodissociation rate constant, J_{IO}, for solar zenith angles of 0°–40° was calculated to have a value of 0.06 ± 0.01 s^{-1}. This value is a factor of 5 lower than previous estimates. Finally, the rate coefficient for the reaction IO + IO → products (3) has been measured at 760 Torr of N_2 and 300 K. The measured effective bimolecular rate constant was found to be $(6.6 \pm 2) \times 10^{-11}$ cm^3·molecule^{-1}·s^{-1}, in good agreement with recent results by Sander (1986).

Introduction

The role of iodine in tropospheric photochemistry has been the subject of speculation for several years.[1-3] It has been proposed, for example, that methyl iodide as well as iodine in other chemical forms from marine sources or nuclear reactors can be photolyzed in the atmosphere to produce atomic iodine. It is further postulated that in the natural troposphere atomic iodine may participate in free radical driven chemical cycles that alter tropospheric levels of ozone, H_xO_y, and NO_x species.[3] Concerning the possible accidental release from nuclear reactors, the question posed is that concerning the atmospheric lifetime of radioactive iodine, and hence, its dispersal over large geographical areas via atmospheric transport processes.

The IO molecule has been identified as one of the key intermediates in the atmospheric iodine cycle;[3,7,8] thus, both its photolytic and gas kinetic lifetime are in need of careful evaluation. The solar photolysis of IO occurs primarily via the $A^2\Pi \leftarrow X^2\Pi$ band system in the 417–470-nm spectral range. This system was discovered[4] and analyzed[5,6] previous to 1961. However, no absolute photoabsorption cross section data were available until a low-resolution spectrum was published in 1983.[7] Subsequently, the latter result has been substantially revised.[8] The present work includes an independent measurement, at higher resolution, that confirms the original study by Cox and Coker[7] while differing somewhat in the relative band intensities, particularly in regard to the (0,0) transition. The rotationally resolved (2,0) band spectrum presented here also supports the J-dependent predissociation suggested by a recent laser-induced fluorescence measurement.[9]

Experimental Section

Iodine monoxide was photochemically generated in this study by the laser flash photolysis of ozone in the presence of iodine. The source mixture was prepared by mixing two flows of nitrogen carrier gas: one that had been passed through a trap containing reagent grade iodine crystals and the other that had been doped with zero grade air and passed through a discharge-type ozone generator. The ozone and iodine concentrations were monitored via optical absorption at 254 nm ($\sigma = 1.13 \times 10^{-17}$ cm^2, ref 10) and 500 nm ($\sigma = 2.19 \times 10^{-18}$ cm^2, ref 11), respectively. As shown in Figure 1, optical absorption measurements of IO were recorded using the output of a XeCl excimer pumped dye laser. The dye laser output bandwidth was approximately 0.01 nm (fwhm). The analysis beam was typically passed through the sample chamber 60 times using a White cell[15] configuration; however, the actual number of passes was limited by films forming on the AR coated chamber windows, presumably due to thermal reactions of the type

$$I_2 + O_3 \rightarrow \text{products}$$

The photolysis laser consisted of a KrF excimer laser which produced 30 mJ per pulse at 248 nm in a 12 mm × 12 mm beam. For absolute cross section measurements, the beam was apertured to 10 mm × 10 mm. The spatial homogeneity of the beam was verified by scanning a pinhole aperture across the beam profile and by inspecting burn patterns on photosensitive paper. Spatial variations were 10% or less. The photolysis energy was measured by a calibrated thermopile (Scientech) that was positioned immediately behind the sample cell. These raw measurements were then corrected for Fresnel losses by using the measured transmissivity of the cell. Absorption of the photolysis beam by the sample gas was found to be negligible.

† Current address: Atlanta University Center, DEMSRI, 440 Westview Drive, S.W., Atlanta, GA 30310.
‡ Current address: Molecular Sciences Branch, Georgia Tech Research Institute, Atlanta, GA 30332.

(1) Moyers, J. L.; Duce, R. A. *J. Geophys. Res.* **1972**, *77*, 5229.
(2) Zafiriou, O. C. *J. Geophys. Res.* **1974**, *79*, 2730.
(3) Chameides, W. L.; Davis, D. D. *J. Geophys. Res. A* **1980**, *85*, 7383.
(4) Vaidya, W. M. *Proc.-Indian Acad. Sci., Sect. A* **1937**, *6A*, 122.
(5) Coleman, E. H.; Gaydon, A. G.; Vaidya, W. M. *Nature (London)* **1948**, *162*, 108.
(6) Durie, R. A.; Legay, F.; Ramsay, D. A. *Can. J. Phys.* **1960**, *38*, 444.
(7) Cox, R. A.; Coker, G. B. *J. Phys. Chem.* **1983**, *87*, 4478.
(8) Jenkin, M. E.; Cox, R. A. *J. Phys. Chem.* **1985**, *89*, 192.
(9) Inoue, G.; Suzuki, M.; Washida, N. *J. Chem. Phys.* **1983**, *79*, 4730.
(10) Griggs, M. J. *J. Chem. Phys.* **1968**, *49*, 857.
(11) Tellinghuisen, J. *J. Chem. Phys.* **1973**, *58*, 2821.
(12) Hesstvedt, E.; Hov, O.; Isaksen, I. S. A. *Int. J. Chem. Kinet.* **1978**, *10*, 971.
(13) Ray, G. W.; Watson, R. T. *J. Phys. Chem.* **1981**, *85*, 2955.
(14) "Chemical Kinetic and Photochemical Data for use in Stratospheric Modeling—Evaluation Number 4: NASA Panel for Data Evaluation"; JPL, Publication 81-3; Jet Propulsion Laboratory, California Institute of Technology: Pasadena, CA, 1981.
(15) White, J. U. *J. Opt. Soc. Am.* **1942**, *32*, 285.

0022-3654/88/2092-1862$01.50/0